SCIENTIFIC REPORTS

OPEN

Spurious violation of the Stokes–Einstein–Debye relation in supercooled water

Received: 18 February 2019
Accepted: 17 May 2019
Published online: 31 May 2019

Takeshi Kawasaki[1] & Kang Kim[2,3]

The theories of Brownian motion, the Debye rotational diffusion model, and hydrodynamics together provide us with the Stokes–Einstein–Debye (SED) relation between the rotational relaxation time of the ℓ-th degree Legendre polynomials τ_ℓ, and viscosity divided by temperature, η/T. Experiments on supercooled liquids are frequently performed to measure the SED relations, $\tau_\ell k_B T/\eta$ and $D_t\tau_\ell$, where D_t is the translational diffusion constant. However, the SED relations break down, and its molecular origin remains elusive. Here, we assess the validity of the SED relations in TIP4P/2005 supercooled water using molecular dynamics simulations. Specifically, we demonstrate that the higher-order τ_ℓ values exhibit a temperature dependence similar to that of η/T, whereas the lowest-order τ_ℓ values are decoupled with η/T, but are coupled with the translational diffusion constant D_t. We reveal that the SED relations are so spurious that they significantly depend on the degree of Legendre polynomials.

Characterization of the translational and rotational motions of molecules in liquid states is of great significance[1–3]. For this purpose, various transport properties, such as shear viscosity, translational diffusion constant, and rotational relaxation time have been measured both experimentally, and through molecular dynamics (MD) simulations. These properties also play crucial roles in the understanding of the detailed mechanism of hydrogen-bond network dynamics in liquid water[4–11].

The Stokes–Einstein (SE) relation is one of the important characteristics of the translational diffusion constant, D_t, in many liquid state systems, $D_t = k_B T/(6\pi\eta R)$, where k_B, T, η represent the Boltzmann constant, the temperature, and the shear viscosity, respectively. This SE relation is derived originally from the theories of hydrodynamics and Brownian motion, where a rigid spherical particle with a radius R is assumed to be perfectly suspended in a Stokes flow of a constant shear viscosity η under the stick boundary condition[12]. Thus, R is conventionally regarded as the effective hydrodynamic radius of the molecule when applying the SE relation to molecular liquids[13].

Analogous to translational motion, the rotational Brownian motion leads to another SE relation between the rotational diffusion constant, D_r, and η as $D_r = k_B T/(8\pi\eta R^3)$. Based on the Debye model, D_r can also be determined by solving the rotational diffusion equation for the reorientation of the molecular dipole as $D_r = 1/[\tau_\ell \ell(\ell+1)]$, where τ_ℓ is the rotational relaxation time of the ℓ-th order Legendre polynomials[14]. τ_1 and τ_2 are the most-commonly investigated; they are characterized by dielectric relaxation and NMR spectroscopies, respectively. Note that a deviation from $\tau_1/\tau_2 = 3$ has been reported in supercooled molecular liquids, which is regarded as a sign of the breakdown of the Debye model[15–17]. Those two equations result in the Stokes–Einstein–Debye (SED) relation,

$$\frac{\tau_\ell k_B T}{\eta} = \frac{8\pi R^3}{\ell(\ell+1)}. \quad (1)$$

The SED relation can also be expressed as

[1]Department of Physics, Nagoya University, Nagoya, 464-8602, Japan. [2]Division of Chemical Engineering, Graduate School of Engineering Science, Osaka University, Toyonaka, Osaka, 560-8531, Japan. [3]Institute for Molecular Science, Okazaki, Aichi, 444-8585, Japan. Takeshi Kawasaki and Kang Kim contributed equally. Correspondence and requests for materials should be addressed to T.K. (email: kawasaki@r.phys.nagoya-u.ac.jp) or K.K. (email: kk@cheng.es.osaka-u.ac.jp)

$$D_t\tau_\ell = \frac{4R^2}{3\ell(\ell+1)}, \tag{2}$$

by combining further with the SE relation between D_t and η/T. This SED relation is proportional to the quotient D_t/D_r, which accounts for the coupling between the translational and rotational diffusion dynamics at any temperature.

The violation of the SE relation between D_t and η has been intensively observed in various glass-forming liquids, such as *o*-terphenyl[18–23]. In particular, the quantity $D_t\eta/T$ increases towards the glass transition temperature, but exhibits a constant value at high temperatures. These experiments indicate that the translational diffusion occurs in a more enhanced manner than estimations using shear viscosity. Many theoretical efforts have therefore been devoted to explaining the violation of the SE relation in glass-forming liquids[24–32]. MD simulations have also been variously performed to address their molecular mechanisms[33–39]. It is commonly argued that the violation of SE relation is a sign of spatially heterogeneous dynamics and of the non-Gaussian property of the particle displacement distribution[22,40].

The validity of the SED relation is still highly controversial, because there are three possible candidates, $\tau_\ell T/\eta$, $D_t\tau_\ell$, and D_t/D_r, that need to be quantified. Recently, the D_r of supercooled molecular liquids has been calculated using MD simulations following the Einstein relation for rotational Brownian motions[41–43]. Experimental analogs have also been reported using optical spectroscopy in colloidal glasses[44,45]. In particular, it has been shown that the temperature dependences of $D_t\tau_2$ and D_t/D_r are completely different in *o*-terphenyl liquids[42] and diatomic molecular liquids[43]; D_t/D_r significantly decreases with decreasing temperature, indicating the translational-rotational decoupling. In contrast, $D_t\tau_2$ exhibits the opposite temperature dependence, *i.e.*, increases in τ_2 exceed the time scale of the translational diffusion constant, $1/D_t$, as the temperature decreases. This discrepancy is thus attributed to the inconsistency between the two expressions, Eqs (1) and (2). However, the direct measurement of R is impractical for molecular liquids both in experiments and MD simulations. More practically, the breakdown of the Debye model, *i.e.*, the ℓ dependence of τ_ℓ, prevents us from making a precise assessment of the SED relation, whichever one of three quantities is utilized.

For liquid water, it has been widely accepted that the validity of the Debye model for molecular reorientation is limited even in normal states, although that is frequently used when analyzing experimental data. Instead, various large-amplitude rotational jump models have been developed to give an accurate prediction of the rotational relaxation time τ_2[7,8,11]. Particularly for supercooled water, the appropriate description for the violation of the SED relation becomes more complicated. Recent MD simulations have demonstrated that the translational and rotational dynamics become spatially heterogeneous upon cooling[46,47]. Furthermore, the violations of the SE and SED relations have been intensely characterized through both experiments and simulations[11,48–67]. In particular, the violation of the SED relation and the translational-rotational decoupling in supercooled water have been reported by calculating D_t and D_r, while η has not been calculated[49,52,57], despite the fact that η plays an essential role in the precise assessment of the SE relation[60–63]. The SED relation has been investigated by calculating the η of SPC/E supercooled water, during which D_r was not calculated[62]. Under these conditions, the SED relation, particularly for the ℓ dependence of $\tau_\ell T/\eta$, has not yet been thoroughly investigated, while only one experimental data analysis has been conducted for $\tau_2 T/\eta$[59].

The purpose of this study is to shed light on the controversy regarding the violation of the SED relation, specifically through the numerical calculations of three quantities, $\tau_\ell T/\eta$, $D_t\tau_\ell$, and D_t/D_r. In particular, we aim to demonstrate that the ℓ dependence of $\tau_\ell T/\eta$ is an important factor in exploring the inherent translational-rotational dynamics in supercooled water.

Results

Here we examine the translational and rotational SE relations, $D_t \propto \eta/T$ and $D_r \propto \eta/T$, respectively. We determined D_t and D_r from the long-time behaviors of the translational and rotational mean-square displacements, respectively (see Methods). We calculated η using the Green–Kubo formula for the shear stress correlation function, as detailed in a previous study[63]. Figure 1(a) shows both D_t and D_r as a function of η/T. Comparing these with the dashed line representing the linear relationship, we find that both the translational and the rotational SE relations are invalid in supercooled regimes, particularly at $T < 250$ K. Note that the rotational SE relation is violated to a greater extent than the translational SE relation. Figure 1(b) shows the ratio of the translational and rotational diffusion constants, D_t/D_r, as a function of the scaled inverse of temperature. The substantial decoupling displayed between the two diffusion constants indicates that the translational and rotational dynamics are decoupling, which is comparable with the previously reported results on ST2[49], SPC/E[52], and TIP4P/2005[57] models. Furthermore, similar results are also demonstrated in *o*-terphenyl liquids[42] and diatomic molecular liquids[41,43] using MD simulations.

The observed decoupling of translational-rotational diffusion is directly related to the inconsistency regarding the effective hydrodynamic radius observed when using the SE relations. We quantified the hydrodynamic radius for the translational degree of freedom, $R_t = k_B T/(6\pi\eta D_t)$, and the rotational counterpart, $R_r = [k_B T/(8\pi\eta D_r)]^{1/3}$. Figure 1(c) shows the temperature dependences of R_t and R_r. At $T = 300$ K, R_t and R_r are approximated by 1.2 Å and 1.0 Å, respectively. These values are slightly smaller than the van der Waals radius of the TIP4P/2005 model. As seen in Fig. 1(c), these two radii sharply decrease upon supercooling, accompanied by violation of the translational and rotational SE relations. Moreover, the difference between R_t and R_r increases with decreasing the temperature, implying that the translational and rotational diffusions are decoupling. The relevance of the decoupling D_t/D_r will be discussed below.

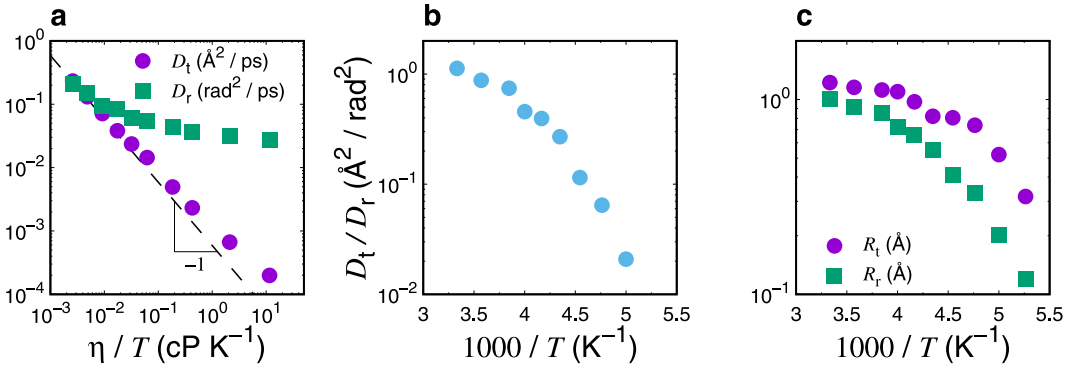

Figure 1. (**a**) Assessments of the translational and rotational SE relations, $D_t\eta/T$ and $D_r\eta/T$, made by plotting the relationships between the translational diffusion constant D_t or the rotational diffusion constant D_r and the shear viscosity divided by the temperature η/T. The dashed line represents the linear relation $D_{t,r} \propto \eta/T$, which represents the SE relation. Neither the translational nor the rotational SE relations are satisfied in supercooled region ($T < 250$ K). (**b**) Temperature dependence of the ratio of rotational and translational diffusion constants, D_r/D_t. As T decreases, this ratio increases, indicating the translational-rotational diffusion decoupling. (**c**) Temperature dependence of translational and rotational hydrodynamic radii, R_t and R. Both R_t and R_r decrease significantly upon cooling, accompanied with violation of SE relations. In particular, upon cooling, R_r decreases at a higher rate than that of R_t in response to decreasing temperature.

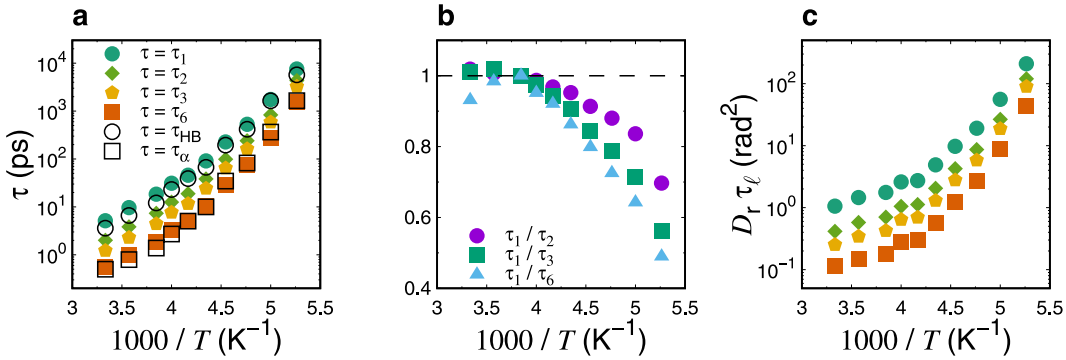

Figure 2. (**a**) Temperature dependence of ℓ-th order rotational relaxation times τ_ℓ for $\ell = 1$, 2, 3, and 6. The temperature dependences of hydrogen-bond lifetime, τ_{HB}, and α-relaxation time, τ_α, are included for comparison. (**b**) Temperature dependence of ratio τ_1/τ_2, τ_1/τ_3, and τ_1/τ_6. Each quantity is scaled by the value at $T = 260$ K. (**c**) Assessments of the Debye model, made by plotting the temperature dependence of $D_r\tau_\ell$ for $\ell = 1$, 2, 3, and 6.

Next, we investigate τ_ℓ as determined from the ℓ-th order Legendre polynomials, and explore its relationship with D_r. Figure 2(a) shows τ_ℓ (for $\ell = 1$, 2, 3, and 6) as a function of the scaled inverse of the temperature. τ_ℓ increases for all ℓ values as the temperature decreases. Interestingly, we observe that τ_ℓ values with higher-order degrees exhibit stronger temperature dependence than those of the lowest order. In other words, the ratios τ_1/τ_2, τ_1/τ_3, and τ_1/τ_6 notably decrease as the temperature decreases (see Fig. 2(b)). A similar result was found using MD simulations of the SPC/E supercooled water[62]. As evident in Fig. 2(b), $D_r\tau_\ell$ exhibits strong temperature dependence, indicating the breakdown of the Debye model. The observed deviation increases for higher-order ℓ values with decreasing temperatures. The breakdown of the Debye model and the inconsistency between R_t and R_r in supercooled states suggest that the SED relations, $\tau_\ell T/\eta$, $D_t\tau_\ell$, and D_t/D_r, are likely spurious quantities. More precisely, these quantities cannot represent real translational and rotational dynamics in supercooled water, regardless of whether they exhibit anomalous deviations from values at high temperatures. We below demonstrate ambiguities of the SED relations, of which results markedly depend on the order ℓ.

Here, we address the SED relation $\tau_\ell T/\eta$, which is the counterpart to recent experimental data[59]. Figure 3(a) shows the relationship between η/T and τ_ℓ for $\ell = 1$ and $\ell = 6$. Note that the results of $\ell = 2$ and $\ell = 3$ are omitted from the plot to improve its clarity. As observed in Fig. 3(a), τ_1 deviates from the value predicted by the SED relation, particularly at lower temperatures ($T < 250$ K), instead exhibiting the fractional form $\tau_1 \propto (\eta/T)^{-0.8}$. In contrast, τ_ℓ with at higher-order $\ell = 6$ follows the SED relation, $\tau_6 \propto \eta/T$. Figure 3(b) shows the temperature dependence of $\eta/(\tau_\ell T)$ (for $\ell = 1$ and $\ell = 6$), in comparison with that of the translational SE relation, $D_t\eta/T$. We observe that the temperature dependence of $\eta/(\tau_1 T)$ is analogous to that of $D_t\eta/T$, suggesting the violation of the

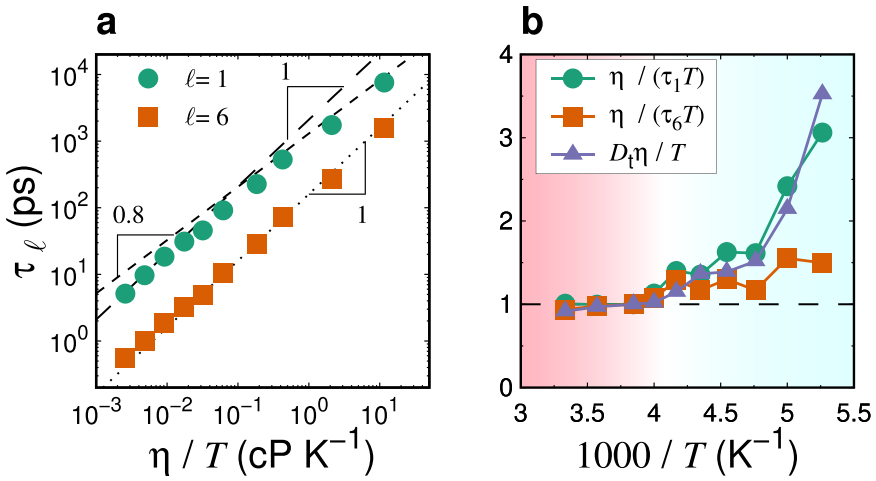

Figure 3. (**a**) Assessments of the SED relation, $\tau_\ell T/\eta$, made by plotting the relationships between rotational relaxation time τ_ℓ for $\ell = 1$ and $\ell = 6$, and the shear viscosity divided by the temperature, η/T. Both the dotted line and the long-dashed line represent the SED relation, $\tau_\ell \propto \eta/T$. The short-dashed line represents $\tau_\ell \propto (\eta/T)^{0.8}$. (**b**) Assessments of the SED relation, $\tau_\ell T/\eta$, made by plotting the temperature dependence of $\eta/(\tau_\ell T)$ for $\ell = 1$ and $\ell = 6$. The violation of the SE relation, $D_t\eta/T$, is also plotted for comparison. Each quantity is scaled by the value at $T = 260$ K. The SED ratio $\eta/(\tau_1 T)$ exhibits a temperature dependence similar to the violation of the SE relation, $D_t\eta/T$, whereas the plot of $\eta/(\tau_6 T)$ resembles the SED relation, Eq. (1). The background color (white region) indicates the onset temperature of the SE violation.

SE relation, whereas $\eta/(\tau_6 T)$ exhibits a weaker temperature dependence. We previously demonstrated the relationship $\tau_\alpha \propto \eta/T$ in TIP4P/2005 supercooled water[63]. Here, τ_α denotes the α-relaxation time that was determined from the incoherent intermediate scattering function $F_s(k, t)$. The wave-number, k, was chosen as $k = 3.0$ Å^{-1}, which corresponds to the main peak of the static structure factor of oxygen, $S_{OO}(k)$. This implies that $D_t\tau_\alpha$ is a good proxy for the translational SE relation $D_t\eta/T$. Similar results have also been reported for other supercooled liquid systems[34,38,39,68]. Accordingly, the temperature dependence of τ_ℓ with higher-order ℓ resembles the coupling with that of τ_α (see Fig. 2(a)). On the other hand, the deviation of $\eta/(\tau_1 T)$ from this value at high temperatures superimposes the violation of the translational SE relation, $D_t\eta/T$ or $D_t\tau_\alpha$.

We next examine the second SED relation, $D_t\tau_\ell$. Figure 4(a and b) display the relationship between D_t and τ_ℓ and the temperature dependence of $D_t\tau_\ell$, respectively. As τ_6 can serve as a proxy of η/T as observed in Fig. 3, $D_t\tau_6$ exhibits a comparable temperature dependence with the SE ratio $D_t\eta/T$ (see Fig. 4(b)). In contrast, τ_1 exhibits a temperature dependence similar to that of D_t. Furthermore, we show an alternative quantity, $D_t\tau_{HB}$, with the hydrogen-bond lifetime, τ_{HB}. Here, τ_{HB} represents the time scale characterizing the irreversible hydrogen-bond breakage process, which is determined from the hydrogen-bond correlation function[69–73]. As demonstrated in a previous study and displayed in Fig. 4(b), the SE relation is preserved as $D_t \sim \tau_{HB}^{-1}$ if the time scale τ_α is replaced with τ_{HB}[63]. Similar observations have also been reported in binary soft-sphere supercooled liquids[74] and silica-like network-forming supercooled liquids[68]. This SE preservation is understood by a possible "jump model". As outlined in the ref.[63], the frequency of the jump motion can be represented as $f \sim 1/\tau_{HB}$ at investigated temeperatues. Correspondingly, the translational diffusion constant is modeled as $D_t \sim \ell_{jump}^2 f \sim \ell_{jump}^2/\tau_{HB}$, where ℓ_{jump} denotes a typical jump length (~Å). Therefore, $D_t\tau_{HB}$ becomes constant. This SE preservation indicates that irreversible hydrogen-bond breakages destroy the local tetrahedral structures, and lead to the translational and rotational molecular jumps with high mobility. It also implies the the coupling between τ_1 and τ_{HB}, which is demonstrated in Fig. 4.

To elucidate the molecular mechanism of the demonstrated relationship between D_t and τ_ℓ, we analyze the generalized van Hove self correlation function, *i.e.*, the joint probability distribution function for the translational displacement and the rotational angle of the molecule, $G_s(\vec{r}, \theta; t) = (1/N)\sum_{j=1}^{N}\langle\delta(\vec{r} - \Delta\vec{r}_j(t))\delta(\theta - \Delta\theta_j(t))\rangle$[75]. Here, $\Delta\vec{r}_j(t)$ and $\Delta\theta_j(t)$ are the translational displacement vector of oxygen and the rotational angle of the dipole moment of a molecule j during a time t, respectively. Figure 5 shows the contour maps of $4\pi r^2 G_s(r, \theta; t)$ with $r = |\vec{r}|$ for $t = 0.1$ ps, 1 ns, and 10 ns at $T = 190$ K. For the shorter time interval, $t = 0.1$ ps, the distribution is stretched towards the rotational angle direction, θ, which is caused by the libration motion of the molecule. This observation corresponds to the oscillations of $C_\ell(t)$ (see Supplementary Fig. S2). At longer time scales, however, $G_s(r, \theta; t)$ shows the coupling between the translational displacement and the rotational angle, which is consistent with the previously reported results of ref.[75]. Furthermore, the broad ridge separated from the main peak denotes the non-Gaussianity of $G_s(r, \theta; t)$. A tagged molecule is trapped by a cage composed of neighbor molecules for longer times in supercooled regime. The rotational relaxation time τ_1, of which the characteristic angle is $\pi/2$ rad, is governed by this large rotational mobility. The single molecule eventually begins diffusion by escaping from the

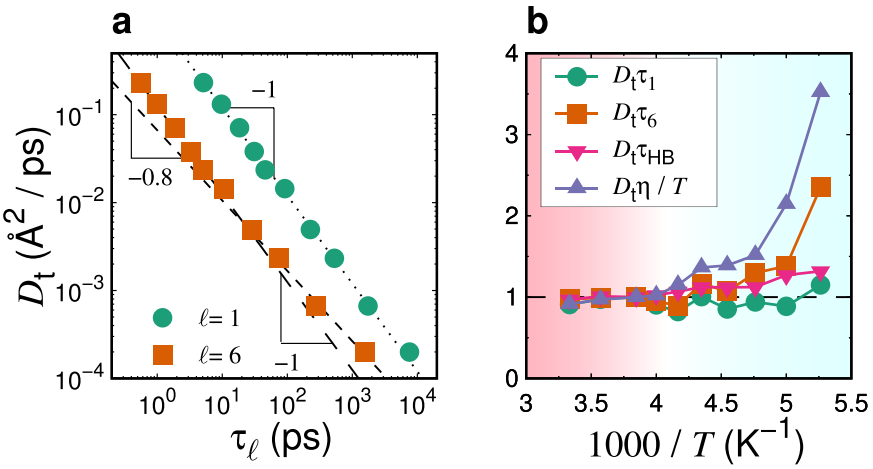

Figure 4. (**a**) Assessments of the SED relation, $D_t\tau_\ell$, made by plotting the relationship between the translational diffusion constant, D_t, and the rotational relaxation time, τ_ℓ, for $\ell = 1$ and $\ell = 6$. Both the dotted line and the long-dashed line represent the SED relation, $D_t \propto \tau_\ell^{-1}$. The short-dashed line represents $D_t \propto \tau_\ell^{-0.8}$. (**b**) Assessments of the SED relation, $D_t\tau_\ell$, made by plotting the temperature dependence of the SED ratios $D_t\tau_\ell$. The violation of SE relation, $Dt\eta/T$, is also plotted for comparison. $D_t\tau_{HB}$, with hydrogen-bond lifetime τ_{HB}, is also shown. Each quantity is scaled by the value at $T = 260$ K. Note that $D_t\tau_{HB}$ shows the preservation of the SE relation[63]. The SED ratio $\eta/(\tau_1 T)$ exhibits a temperature dependence similar to the preservation of the SE relation, $D_t\tau_{HB}$, whereas $D_t\tau_6$ bears a certain resemblance to the violation of the SE relation, $D_t\eta/T$. The background color (white region) indicates of the onset temperature of the SE violation.

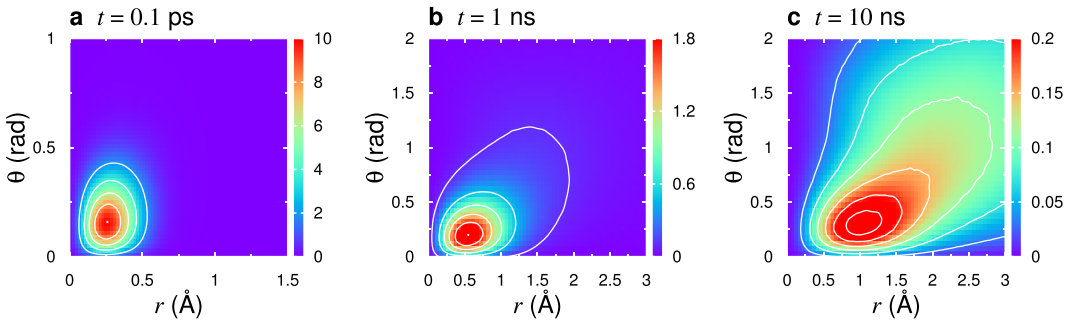

Figure 5. Joint probability distribution functions (generalized van Hove correlation function) $4\pi r^2 G_s(r, \theta; t)$ for $t = 0.1$ ns, 1 ns, and 10 ns at $T = 190$ K. The value of the color bar is normalized by Å^2. Remarkable positive correlations between translational displacement $|\Delta\vec{r}_j(t)|$ and rotational angle $\Delta\theta_j(t)$ are observed, particularly for large r and θ values. This indicates that a large translational motion correlates with a large rotational motion of molecule.

cage, utilizing large translational and rotational mobilities. Thus, τ_1 is regarded as the time scale coupled with D_t. In addition, the time scale of τ_1 is similar to the hydrogen-bond lifetime τ_{HB}, as demonstrated in Fig. 2(a).

In contrast, the relaxation time τ_6 corresponds to a molecular reorientation with an angle of 0.37 rad, which lies near to the dominant peak of $G_s(r, \theta; t)$ at $t = 10$ ns (see Fig. 5(c)). The higher-order ℓ mostly highlights immobile molecules both for translational and rotational motions, which will contribute to the dynamical heterogeneities. To investigate this, we characterize the dynamic heterogeneity of translational and rotational motions using the four-point correlation functions, $\chi_{t,r}(t)$ (see Methods and Supplementary Fig. S3(a)). We found that the time scale τ_6 is akin to the peak time of $\chi_{t,r}(t)$, which shows that its temperature dependence is similar to that of τ_α (see Supplementary Fig. S3(b)). Consequently, the similar temperature dependences between τ_6 and τ_α are demonstrated in Fig. 2(a).

Finally, we discuss the strong decoupling behavior of the translational and rotational diffusion constants, as demonstrated in Fig. 1. As already pointed out in ref.[8], the use of the rotational diffusion constant D_r needs particular care due to the limitation of the angular Brownian motion scnenario. Furthermore, it has been revealed that D_r is superfacial for describing the reorientational motion in supercooled molecular liquids[43]. The angular mean-square displacement $\langle\Delta\phi(t)^2\rangle$ is largely influenced by the accumulation of the libration motion, which has a time scale of 0.1 ps. Each molecule can rotate, despite being trapped by the cage, at this short time scale, as indicated in Fig. 5(a). Accordingly, the angular mean-square displacement exhibits a plateau, but its persistent time is much smaller than that of $C_\ell(t)$, particularly at lower temperatures (See Supplementary Figs S1 and S2). In

contrast, the plateau of $C_\ell(t)$ after the time scale of libration motion indicates the occurrence of the cage effect (see Supplementary Fig. S2). These findings imply that the decoupling between D_t and D_r has no direct relevance to the real translational-rotational coupling, $D_t \propto \tau_1^{-1}$. This translational-rotational coupling scenario is in accord with the observation in supercooled molecular liquids[43].

Discussion

In this paper, we report the numerical results of MD simulations of the relationship between the translational and rotational dynamics in TIP4P/2005 supercooled liquid water. Our contributions to the assessment of translational and rotational SE relations and the Debye model can be summarized as follows:

(i) Both translational and rotational SE relations, $D_t \propto (\eta/T)^{-1}$ and $D_r \propto (\eta/T)^{-1}$, are significantly violated in supercooled states. In particular, the rotational SE relation is violated stronger to a greater extent than that of translational SE relation. Correspondingly, the rotational hydrodynamic radius becomes significantly smaller than translational one with decreasing temperature.

(ii) We test the validity of the Debye model, $D_r \propto \tau_\ell^{-1}$, for the orders $\ell = 1, 2, 3$, and 6 of the Legendre polynomials, demonstrating that the rotational relaxation time τ_ℓ is entirely inconsistent with the rotational diffusion constant D_r.

(iii) Furthermore, we systematically examine the SED relations $\tau_\ell T/\eta$ and $D_t\tau_\ell$. We reveal that these SED relations strongly depend on the order of ℓ, leading to the following spurious argument: The SED relation $\tau_\ell \propto \eta/T$ is violated with the lowest-order rotational relaxation time τ_1, but is instead satisfied at the higher-order time scale of τ_6. In contrast, we find that $D_t\tau_6$ deviates from values at high temperatures, similarly to the violation of the translational SE relation $D_t\eta/T$, while $D_t\tau_1$ superficially satisfies the SED relation.

(iv) We observe the coupling between the translational diffusion constant, D_t, and the lowest rotational relaxation time, τ_1. We characterize the correlation between large translational and rotational mobilities using from the van Hover correlation function $G_s(r, \theta; t)$. Furthermore, we find that τ_1 exhibits the temperature dependence similar to that of the hydrogen-bond lifetime τ_{HB}, which is consistent with the previously demonstrated result, $D_t \propto {\tau_{HB}}^{-1}$[63].

(v) On the contrary, we show that the higher-order rotational relaxation time τ_6 is analogous with the α-relaxation time τ_α, rather than with τ_{HB}. This time scale is characterized by immobile molecular mobilities showing dynamic heterogeneities, which we investigate using the four-point correlation functions $\chi_t(t)$ and $\chi_r(t)$. It is also of essential to examine the role of the length scale of dynamic heterogeneities ξ_4 on the violations of the SE/SED relations in supercooled water. The ξ_4 value is conventionally quantified by the wave-number dependence of the four-point correlation functions[76]. This calculation necessitates MD simulations using more substantial large systems, which are currently undertaken.

(vi) In conclusion, in this paper we provide significant and unprecedented insights into the appropriate assessment of SE, Debye, and SED relationships, in doing so clarifying previously awkward and confusing contradictions. Finally, it is worth mentioning the importance of the density dependence on the SE/SED relations in supercooled water. In fact, both η and D_t show anomalous density dependence, particularly at low temperaures[65]. Further investigations along this line are necessary to clarify this issue.

Methods

Molecular dynamics simulations. We performed MD simulations of liquid water using the Large-scale Atomic/Molecular Massively Parallel Simulator (LAMMPS)[77], and used the TIP4P/2005 model to calculate the water molecule potentials[78]. Other MD simulations were also carried out to investigate various properties in supercooled states of this model[65–67,79–86]. The comparison with other rigid non-poralizable models was also made in the recent review[87]. Remark that recent ab initio MD simulations provide a more realistic behavior of the dynamics in supercooled regime[88]. We used a Coulombic cutoff 1 nm. The particle-particle particle-mesh solver was utilized to calculate long-range Coulomb interactions, and the SHAKE algorithm was also used for bond and angle constraints. Periodic boundary conditions were used, and the time step of simulation was 1 fs. First, we employed the *NVT* ensembles for $N = 1{,}000$ water molecules was employed at various temperatures ($T = 300$, 280, 260, 250, 240, 230, 220, 210, 200, and 190 K) with a fixed mass density of $\rho = 1\,\mathrm{g\,cm^{-3}}$. The corresponding system size was $L = 31.04$ Å. We conducted the *NVE* ensemble simulations after the equilibration with a sufficient long time at each temperature, The dynamical quantities including, the α-relaxation time τ_α, the translational diffusion constant D_t, and the hydrogen-bond lifetime τ_{HB}, and shear viscosity η used in here are reported in a previous study[63]. In this study, we newly calculated time correlation functions for characterzing the rotational diffusion constant D_r, the rotational relaxation time of the ℓ-th degree Legendre polynomials τ_ℓ. Furthermore, the four-point correlation function was also calculated for characterizing dynamic heterogeneities of rotational molecular motions. The trajectories for the calculations of various quantities were for 10 ns ($T \geq 220$ K) and 100 ns ($T \leq 210$ K). We average over five independent simulation runs for the calculations.

Rotational diffusion constant and rotational relaxation time. We calculated the angular mean-square displacement $\langle \Delta\phi(t)^2 \rangle = (1/N)\sum_{j=1}^{N} \langle |\Delta\vec{\phi}_j(t)|^2 \rangle$, following ref.[52] (see Supplementary Fig. S1(a)). We obtained the angular displacement vector $\Delta\vec{\phi}_j(t)$ of the molecule j is obtained through the time integration of the angular velocity vector, $\vec{\phi}_j(t) = \int_{t'}^{t'+t} \vec{\omega}_j(t)\mathrm{d}t$, where the angular velocity vector $\vec{\omega}_j(t)$ of the molecule j is given

by the cross-product of the normalized polarization vector $\vec{e_j}(t)$ as, $\vec{\omega_j}(t) = \vec{e_j}(t) \times \vec{e_j}(t + \Delta t)/\Delta t$, with the magnitude $|\vec{\omega_j}(t)| = \cos^{-1}(\vec{e_j}(t) \cdot \vec{e_j}(t + \Delta t))$. Note that Δt is chosen by a sufficiently small time interval; this was 10 fs in our calculations. We determined the rotational diffusion constant D_r was determined from the long-time limit of $\langle \Delta\vec{\phi}(t)^2 \rangle$ as $D_r = \lim_{t\to\infty} \langle \Delta\phi(t)^2 \rangle/4t$. Furthermore, we independently calculated the angular velocity time correlation function, $C_\Omega(t) = (1/3N)\sum_{j=1}^{N} \langle \vec{\Omega}_j(t) \cdot \vec{\Omega}_j(0) \rangle$, where $\vec{\Omega}_j(t)$ denotes the angular velocity vector of the molecule j in the world reference frame following ref.[57] (see Supplementary Fig. S1(b)). We also used the Green–Kubo formula to obtain D_r as $D_r = \int_0^\infty C_\Omega(t)dt$. We confirmed that the D_r values obtained from these two methods are consistent at any temperature.

The rotational correlation function $C_\ell(t)$ is defined by the autocorrelation function of the normalized polarization vector $\vec{e_j}(t)$ as $C_\ell(t) = (1/N)\sum_{j=1}^{N} \langle P_\ell[\vec{e_j}(t) \cdot \vec{e_j}(0)] \rangle$, where $P_\ell[x]$ is the ℓ-th order Legendre polynomial as a function of x (see Supplementary Fig. S2). $C_\ell(t)$ decays from 1 to 0 as t increases. We obtained the ℓ-th ($\ell = 1, 2, 3$, and 6) order rotational relaxation time τ_ℓ by fitting $C_\ell(t)$ to the Kohlrausch–Williams–Watts function $A\exp\{-(t/\tau_\ell)^{\beta_\ell}\}$.

Rotational four-point correlation functions. We used the four-point correlation function to elucidate the degree of dynamic heterogeneity in supercooled liquids[76]. The four-point correlation $\chi_t(t)$ for translational motions is defined by the variance of the intermediate scattering function $F_s(k, t)$ as, $\chi_t(t) = N[\langle \hat{F}_s(k, t)^2 \rangle - \langle \hat{F}_s(k, t) \rangle^2]$, with $\hat{F}_s(t) = (1/N)\sum_{j=1}^{N} \cos[\vec{k} \cdot \Delta\vec{r_j}(t)]$. We previously calculated $\chi_t(t)$ using the wave-number $k = 3.0$ Å^{-1}, and quantified the peak time τ_t (note that the same quantity was denoted by τ_{χ_4} in ref.[63]). The rotational four-point correlation function $\chi_r(t)$ can be analogously defined as $\chi_r(t) = N[\langle \hat{C}_\ell(t)^2 \rangle - \langle \hat{C}_\ell(t) \rangle^2]$, with $\hat{C}_\ell(t) = (1/N)\sum_{j=1}^{N} P_\ell[\vec{e_j}(t) \cdot \vec{e_j}(0)]$. The peak time of $\chi_r(t)$ is represented by τ_r.

Data Availability

The data supporting the findings of this study are available from the corresponding authors upon reasonable request.

References

1. Berne, B. J. & Pecora, R. *Dynamic Light Scattering: With Applications to Chemistry, Biology, and Physics*. (Dover, New York, 2000).
2. Bagchi, B. *Molecular Relaxation in Liquids*. (Oxford University Press, New York, 2012).
3. Hansen, J. P. & McDonald, I. R. *Theory of Simple Liquids*. 4th edn. (Academic Press, London, 2013).
4. Conde, O. & Teixeira, J. Hydrogen bond dynamics in water studied by depolarized Rayleigh scattering. *J. Phys. France* **44**, 525–529 (1983).
5. Teixeira, J., Bellissent-Funel, M. C., Chen, S. H. & Dianoux, A. J. Experimental determination of the nature of diffusive motions of water molecules at low temperatures. *Phys. Rev. A* **31**, 1913–1917 (1985).
6. Agmon, N. Tetrahedral Displacement: The Molecular Mechanism behind the Debye Relaxation in Water. *J. Phys. Chem.* **100**, 1072–1080 (1996).
7. Laage, D. & Hynes, J. T. A Molecular Jump Mechanism of Water Reorientation. *Science* **311**, 832–835 (2006).
8. Laage, D. & Hynes, J. T. On the Molecular Mechanism of Water Reorientation. *J. Phys. Chem. B* **112**, 14230–14242 (2008).
9. Moilanen, D. E. *et al*. Water inertial reorientation: Hydrogen bond strength and the angular potential. *Proc. Natl. Acad. Sci. USA* **105**, 5295–5300 (2008).
10. Qvist, J., Schober, H. & Halle, B. Structural dynamics of supercooled water from quasielastic neutron scattering and molecular simulations. *J. Chem. Phys.* **134**, 144508 (2011).
11. Qvist, J., Mattea, C., Sunde, E. P. & Halle, B. Rotational dynamics in supercooled water from nuclear spin relaxation and molecular simulations. *J. Chem. Phys.* **136**, 204505 (2012).
12. Landau, L. D. & Lifshitz, E. M. *Fluid Mechanics*. 2nd edition edn. (Pergamon Press, Oxford, 1987).
13. Schmidt, J. R. & Skinner, J. L. Hydrodynamic boundary conditions, the Stokes–Einstein law, and long-time tails in the Brownian limit. *J. Chem. Phys.* **119**, 8062–8068 (2003).
14. Debye, P. J. W. *Polar Molecules*. (Dover, New York, 1929).
15. Kivelson, D. & Miles, D. Bimodal angular hopping model for molecular rotations in liquids. *J. Chem. Phys.* **88**, 1925–1933 (1988).
16. Kivelson, D. & Kivelson, S. A. Models of rotational relaxation above the glass transition. *J. Chem. Phys.* **90**, 4464–4469 (1989).
17. Diezemann, G., Sillescu, H., Hinze, G. & Böhmer, R. Rotational correlation functions and apparently enhanced translational diffusion in a free-energy landscape model for the α relaxation in glass-forming liquids. *Phys. Rev. E* **57**, 4398–4410 (1998).
18. Fujara, F., Geil, B., Sillescu, H. & Fleischer, G. Translational and rotational diffusion in supercooled orthoterphenyl close to the glass transition. *Z. Phys. B* **88**, 195 (1992).
19. Chang, I. *et al*. Translational and rotational molecular motion in supercooled liquids studied by NMR and forced Rayleigh scattering. *J. Non-Cryst. Solids* **172–174**, 248 (1994).
20. Cicerone, M. T. & Ediger, M. D. Enhanced translation of probe molecules in supercooled o-terphenyl: Signature of spatially heterogeneous dynamics? *J. Chem. Phys.* **104**, 7210 (1996).
21. Andreozzi, L., Di Schino, A., Giordano, M. & Leporini, D. Evidence of a fractional Debye-Stokes-Einstein law in supercooled o-terphenyl. *EPL* **38**, 669 (1997).
22. Ediger, M. D. Spatially heterogeneous dynamics in supercooled liquids. *Annu. Rev. Phys. Chem.* **51**, 99–128 (2000).
23. Mapes, M. K., Swallen, S. F. & Ediger, M. D. Self-Diffusion of Supercooled o-Terphenyl near the Glass Transition Temperature. *J. Phys. Chem. B* **110**, 507–511 (2006).
24. Hodgdon, J. & Stillinger, F. Stokes-Einstein violation in glass-forming liquids. *Phys. Rev. E* **48**, 207–213 (1993).
25. Stillinger, F. & Hodgdon, J. Translation-rotation paradox for diffusion in fragile glass-forming liquids. *Phys. Rev. E* **50**, 2064–2068 (1994).
26. Stillinger, F. H. A Topographic View of Supercooled Liquids and Glass Formation. *Science* **267**, 1935–1939 (1995).
27. Tarjus, G. & Kivelson, D. Breakdown of the Stokes–Einstein relation in supercooled liquids. *J. Chem. Phys.* **103**, 3071–3073 (1995).
28. Douglas, J. F. & Leporini, D. Obstruction model of the fractional Stokes–Einstein relation in glass-forming liquids. *J. Non-Cryst. Solids* **235–237**, 137–141 (1998).
29. Xia, X. & Wolynes, P. G. Diffusion and the Mesoscopic Hydrodynamics of Supercooled Liquids. *J. Phys. Chem. B* **105**, 6570–6573 (2001).
30. Jung, Y., Garrahan, J. P. & Chandler, D. Excitation lines and the breakdown of Stokes-Einstein relations in supercooled liquids. *Phys. Rev. E* **69**, 99 (2004).

31. Biroli, G. & Bouchaud, J.-P. Critical fluctuations and breakdown of the Stokes–Einstein relation in the mode-coupling theory of glasses. *J. Phys.: Condens. Matter* **19**, 205101 (2007).
32. Ngai, K. L. Breakdown of Debye-Stokes-Einstein and Stokes-Einstein relations in glass-forming liquids: An explanation from the coupling model. *Philos. Mag. B* **79**, 1783–1797 (2009).
33. Thirumalai, D. & Mountain, R. D. Activated dynamics, loss of ergodicity, and transport in supercooled liquids. *Phys. Rev. E* **47**, 479–489 (1993).
34. Yamamoto, R. & Onuki, A. Heterogeneous diffusion in highly supercooled liquids. *Phys. Rev. Lett.* **81**, 4915–4918 (1998).
35. Kumar, S. K., Szamel, G. & Douglas, J. F. Nature of the breakdown in the Stokes-Einstein relationship in a hard sphere fluid. *J. Chem. Phys.* **124**, 214501 (2006).
36. Köddermann, T., Ludwig, R. & Paschek, D. On the Validity of Stokes-Einstein and Stokes-Einstein-Debye Relations in Ionic Liquids and Ionic-Liquid Mixtures. *ChemPhysChem* **9**, 1851–1858 (2008).
37. Harris, K. R. The fractional Stokes–Einstein equation: Application to Lennard-Jones, molecular, and ionic liquids. *J. Chem. Phys.* **131**, 054503 (2009).
38. Shi, Z., Debenedetti, P. G. & Stillinger, F. H. Relaxation processes in liquids: Variations on a theme by Stokes and Einstein. *J. Chem. Phys.* **138**, 12A526 (2013).
39. Sengupta, S., Karmakar, S., Dasgupta, C. & Sastry, S. Breakdown of the Stokes-Einstein relation in two, three, and four dimensions. *J. Chem. Phys.* **138**, 12A548 (2013).
40. Berthier, L. & Biroli, G. Theoretical perspective on the glass transition and amorphous materials. *Rev. Mod. Phys.* **83**, 587–645 (2011).
41. Kämmerer, S., Kob, W. & Schilling, R. Dynamics of the rotational degrees of freedom in a supercooled liquid of diatomic molecules. *Phys. Rev. E* **56**, 5450–5461 (1997).
42. Lombardo, T. G., Debenedetti, P. G. & Stillinger, F. H. Computational probes of molecular motion in the Lewis-Wahnstrom model for ortho-terphenyl. *J. Chem. Phys.* **125**, 174507 (2006).
43. Chong, S. H. & Kob, W. Coupling and Decoupling between Translational and Rotational Dynamics in a Supercooled Molecular Liquid. *Phys. Rev. Lett.* **102**, 392 (2009).
44. Kim, M., Anthony, S. M., Bae, S. C. & Granick, S. Colloidal rotation near the colloidal glass transition. *J. Chem. Phys.* **135**, 054905 (2011).
45. Edmond, K. V., Elsesser, M. T., Hunter, G. L., Pine, D. J. & Weeks, E. R. Decoupling of rotational and translational diffusion in supercooled colloidal fluids. *Proc. Natl. Acad. Sci. USA* **109**, 17891–17896 (2012).
46. Giovambattista, N., Mazza, M. G., Buldyrev, S. V., Starr, F. W. & Stanley, H. E. Dynamic Heterogeneities in Supercooled Water. *J. Phys. Chem. B* **108**, 6655–6662 (2004).
47. Mazza, M. G., Giovambattista, N., Starr, F. W. & Stanley, H. E. Relation between Rotational and Translational Dynamic Heterogeneities in Water. *Phys. Rev. Lett.* **96**, 057803 (2006).
48. Chen, S.-H. *et al*. The violation of the Stokes-Einstein relation in supercooled water. *Proc. Natl. Acad. Sci. USA* **103**, 12974–12978 (2006).
49. Becker, S. R., Poole, P. H. & Starr, F. W. Fractional Stokes-Einstein and Debye-Stokes-Einstein relations in a network-forming liquid. *Phys. Rev. Lett.* **97**, 055901 (2006).
50. Kumar, P. Breakdown of the Stokes–Einstein relation in supercooled water. *Proc. Natl. Acad. Sci. USA* **103**, 12955–12956 (2006).
51. Kumar, P. *et al*. Relation between the Widom line and the breakdown of the Stokes–Einstein relation in supercooled water. *Proc. Natl. Acad. Sci. USA* **104**, 9575–9579 (2007).
52. Mazza, M. G., Giovambattista, N., Stanley, H. E. & Starr, F. W. Connection of translational and rotational dynamical heterogeneities with the breakdown of the Stokes-Einstein and Stokes-Einstein-Debye relations in water. *Phys. Rev. E* **76**, 031203 (2007).
53. Xu, L. *et al*. Appearance of a fractional Stokes-Einstein relation in water and a structural interpretation of its onset. *Nat. Phys.* **5**, 565–569 (2009).
54. Banerjee, D., Bhat, S. N., Bhat, S. V. & Leporini, D. ESR evidence for 2 coexisting liquid phases in deeply supercooled bulk water. *Proc. Natl. Acad. Sci. USA* **106**, 11448–11453 (2009).
55. Mallamace, F. *et al*. Dynamical Crossover and Breakdown of the Stokes-Einstein Relation in Confined Water and in Methanol-Diluted Bulk Water. *J. Phys. Chem. B* **114**, 1870–1878 (2010).
56. Jana, B., Singh, R. S. & Bagchi, B. String-like propagation of the 5-coordinated defect state in supercooled water: molecular origin of dynamic and thermodynamic anomalies. *Phys. Chem. Chem. Phys.* **13**, 16220–16226 (2011).
57. Rozmanov, D. & Kusalik, P. G. Transport coefficients of the TIP4P-2005 water model. *J. Chem. Phys.* **136**, 044507 (2012).
58. Bove, L. E. *et al*. Translational and Rotational Diffusion in Water in the Gigapascal Range. *Phys. Rev. Lett.* **111**, 185901 (2013).
59. Dehaoui, A., Issenmann, B. & Caupin, F. Viscosity of deeply supercooled water and its coupling to molecular diffusion. *Proc. Natl. Acad. Sci. USA* **112**, 12020–12025 (2015).
60. Guillaud, E., Merabia, S., de Ligny, D. & Joly, L. Decoupling of viscosity and relaxation processes in supercooled water: a molecular dynamics study with the TIP4P/2005f model. *Phys. Chem. Chem. Phys.* **19**, 2124–2130 (2017).
61. Guillaud, E., Joly, L., de Ligny, D. & Merabia, S. Assessment of elastic models in supercooled water: A molecular dynamics study with the TIP4P/2005f force field. *J. Chem. Phys.* **147**, 014504 (2017).
62. Galamba, N. On the hydrogen-bond network and the non-Arrhenius transport properties of water. *J. Phys.: Condens. Matter* **29**, 015101 (2017).
63. Kawasaki, T. & Kim, K. Identifying time scales for violation/preservation of Stokes-Einstein relation in supercooled water. *Sci. Adv.* **3**, e1700399 (2017).
64. Shi, R., Russo, J. & Tanaka, H. Origin of the emergent fragile-to-strong transition in supercooled water. *Proc. Natl. Acad. Sci. USA* **115**, 9444–9449 (2018).
65. Montero de Hijes, P., Sanz, E., Joly, L., Valeriani, C. & Caupin, F. Viscosity and self-diffusion of supercooled and stretched water from molecular dynamics simulations. *J. Chem. Phys.* **149**, 094503 (2018).
66. Saito, S., Bagchi, B. & Ohmine, I. Crucial role of fragmented and isolated defects in persistent relaxation of deeply supercooled water. *J. Chem. Phys.* **149**, 124504 (2018).
67. Saito, S. & Bagchi, B. Thermodynamic picture of vitrification of water through complex specific heat and entropy: A journey through "no man's land". *J. Chem. Phys.* **150**, 054502 (2019).
68. Kawasaki, T., Kim, K. & Onuki, A. Dynamics in a tetrahedral network glassformer: Vibrations, network rearrangements, and diffusion. *J. Chem. Phys.* **140**, 184502 (2014).
69. Rapaport, D. C. Hydrogen bonds in water: Network organization and lifetimes. *Mol. Phys.* **50**, 1151–1162 (1983).
70. Saito, S. & Ohmine, I. Translational and orientational dynamics of a water cluster (H2O)108 and liquid water: Analysis of neutron scattering and depolarized light scattering. *J. Chem. Phys.* **102**, 3566 (1995).
71. Luzar, A. & Chandler, D. Hydrogen-bond kinetics in liquid water. *Nature* **379**, 55–57 (1996).
72. Luzar, A. & Chandler, D. Effect of Environment on Hydrogen Bond Dynamics in Liquid Water. *Phys. Rev. Lett.* **76**, 928–931 (1996).
73. Luzar, A. Resolving the hydrogen bond dynamics conundrum. *J. Chem. Phys.* **113**, 10663 (2000).
74. Kawasaki, T. & Onuki, A. Slow relaxations and stringlike jump motions in fragile glass-forming liquids: Breakdown of the Stokes-Einstein relation. *Phys. Rev. E* **87**, 012312 (2013).

75. Faraone, A., Liu, L. & Chen, S. H. Model for the translation–rotation coupling of molecular motion in water. *J. Chem. Phys.* **119**, 6302–6313 (2003).
76. Toninelli, C., Wyart, M., Berthier, L., Biroli, G. & Bouchaud, J.-P. Dynamical susceptibility of glass formers: Contrasting the predictions of theoretical scenarios. *Phys. Rev. E* **71**, 041505 (2005).
77. Plimpton, S. Fast parallel algorithms for short-range molecular dynamics. *J. Comput. Phys.* **117**, 1–19 (1995).
78. Abascal, J. L. F. & Vega, C. A general purpose model for the condensed phases of water: TIP4P/2005. *J. Chem. Phys.* **123**, 234505 (2005).
79. Abascal, J. L. F. & Vega, C. Widom line and the liquid–liquid critical point for the TIP4P/2005 water model. *J. Chem. Phys.* **133**, 234502 (2010).
80. Sumi, T. & Sekino, H. Effects of hydrophobic hydration on polymer chains immersed in supercooled water. *RSC Adv.* **3**, 12743–12750 (2013).
81. Overduin, S. D. & Patey, G. N. An analysis of fluctuations in supercooled TIP4P/2005 water. *J. Chem. Phys.* **138**, 184502 (2013).
82. De Marzio, M., Camisasca, G., Rovere, M. & Gallo, P. Mode coupling theory and fragile to strong transition in supercooled TIP4P/2005 water. *J. Chem. Phys.* **144**, 074503 (2016).
83. Hamm, P. Markov state model of the two-state behaviour of water. *J. Chem. Phys.* **145**, 134501 (2016).
84. Singh, R. S., Biddle, J. W., Debenedetti, P. G. & Anisimov, M. A. Two-state thermodynamics and the possibility of a liquid-liquid phase transition in supercooled TIP4P/2005 water. *J. Chem. Phys.* **144**, 144504 (2016).
85. Gonzalez, M. A., Valeriani, C., Caupin, F. & Abascal, J. L. F. A comprehensive scenario of the thermodynamic anomalies of water using the TIP4P/2005 model. *J. Chem. Phys.* **145**, 054505 (2016).
86. Handle, P. H. & Sciortino, F. Potential energy landscape of TIP4P/2005 water. *J. Chem. Phys.* **148**, 134505 (2018).
87. Vega, C. & Abascal, J. L. F. Simulating water with rigid non-polarizable models: a general perspective. *Phys. Chem. Chem. Phys.* **13**, 19663 (2011).
88. Morawietz, T., Singraber, A., Dellago, C. & Behler, J. How van der Waals interactions determine the unique properties of water. *Proc. Natl. Acad. Sci. USA* **113**, 8368–8373 (2016).

Acknowledgements

We thank K. Miyazaki, N. Matubayasi, T. Nakamura, and H. Shiba for valuable discussions. This work was partly supported by JSPS KAKENHI Grant Numbers JP15H06263, JP16H06018, JP18H01188, and 19K03767. The numerical calculations were performed at the Research Center of Computational Science, Okazaki, Japan.

Author Contributions

T.K. and K.K. designed research, performed simulations, analyzed data, and wrote the paper.

Additional Information

Supplementary information accompanies this paper at https://doi.org/10.1038/s41598-019-44517-4.

Competing Interests: The authors declare no competing interests.

Publisher's note: Springer Nature remains neutral with regard to jurisdictional claims in published maps and institutional affiliations.